DTU Library

Long term strain behavior of PMMA based polymer optical fibers

Bundalo, Ivan-Lazar; Nielsen, Kristian; Woyessa, Getinet; Bang, Ole

Link back to DTU Orbit

Long term strain behavior of PMMA based polymer optical fibers

Ivan-Lazar Bundalo*[a], Kristian Nielsen [a], Getinet Woyessa [a], Ole Bang[a]

[a]DTU Fotonik, Technical University of Denmark, Ørsteds Plads B343, 2800 Kgs. Lyngby, Denmark

*_ivlab@fotonik.dtu.dk_

ABSTRACT

We are reporting on the viscoelasticity of PMMA based Fiber Bragg Grating (FBG) strain sensors when exposed to repeated sequences of long term strain and relaxation with various duty-cycles. In terms of the FBG wavelength and how it follows the strain cycle, we have shown that in the small strain regime (up to 1%) an elastic-dominated fast relaxing range, which is followed by a mainly viscous relaxation, depends both on the strain level and on the strain duration. For a small ratio of the strain-relax durations, this fast relaxation range stays almost the same. However, with increasing strain duration, for the same relaxation time, this range will be shortened, which might influence the sensing capabilities of the fiber sensor.

Keywords: viscoelasticity, pmma, FBG, strain, sensor

1. INTRODUCTION

While silica based Fiber Bragg Gratings (FBGs) have known mechanical properties and the devices based on silica FBGs are already used in various sensing applications, FBGs made in polymers are still missing substantial information regarding their mechanical properties. Having a higher elastic limit, polymer is a suitable material for a number of sensing applications unreachable to silica. However, due to their viscoelastic nature, polymers are experiencing nonlinear behavior when repeatedly strained and relaxed[1,2]. The high-frequency regime (up to 10 kHz), which could be used for acoustic and vibration sensing, has already been investigated by Stefani *et al.*[3]. However, in certain sensors used in geogrids, smart textiles, and endoscopic manometers, FBG based polymer sensors would be experiencing different levels of strain for various durations of time. For such applications, it is important to know how the fiber relaxes and in particular how any relaxation hysteresis behaves for different amounts of strain and different durations of strain. The interesting quasi-static behavior of polymer FBGs, UV-written under strain and then relaxed, was recently investigated[2,4]. Here we investigate the low-frequency behavior of polymer FBGs not written under strain, where the straining and relaxation takes place in several periods of much less than 1 Hz. To have a better understating of the polymer viscoelasticity and the limits imposed by it, we conducted a series of long term measurements where we exposed the fiber to the several amounts of strain with various time intervals.

2. LONG TERM STRAIN EXPERIMENT

The aim of our long-term strain experiments is to see if for different strain levels and strain durations, there is a safe, fast relaxation range of strain for which we know the FBG sensor reading follows the strain-relaxation cycle without any hysteresis appearing (see Fig. 1). We performed the experiments in a temperature and humidity controlled environment where the temperature change was kept within 2°C and the humidity didn't change for more than 2% RH in each series of experiments. The fiber under investigation was an endlessly single-mode 3-ring PMMA microstructured Polymer Optical Fiber (mPOF) with a hole to pitch ratio of 0.26, and a pitch (the hole to hole distance) of 3.75 μm. The fiber, which was cleaved at about 77°C [5], had an initial length of 14 cm, an initial FBG peak wavelength of 618.7 nm, and was strained to a maximum of 1% to avoid material deformation of high strains.

2.1 Strain of 0.5%

In the first part of the experiment we strained the fiber to 0.5% (corresponding to 0.7 mm), kept it strained for a time T_1 (0.5 minutes at the beginning), and subsequently released it to relax for a time T_2 (5 minutes). We repeated the same procedure (cycle) 10 times to see the evolution of the hysteresis. Upon finishing the sequence of strain-release

measurements, we left the fiber resting relaxed for 2 hours to mitigate any possible accumulated stress. The scheme explaining the procedure is shown in Figure 1.
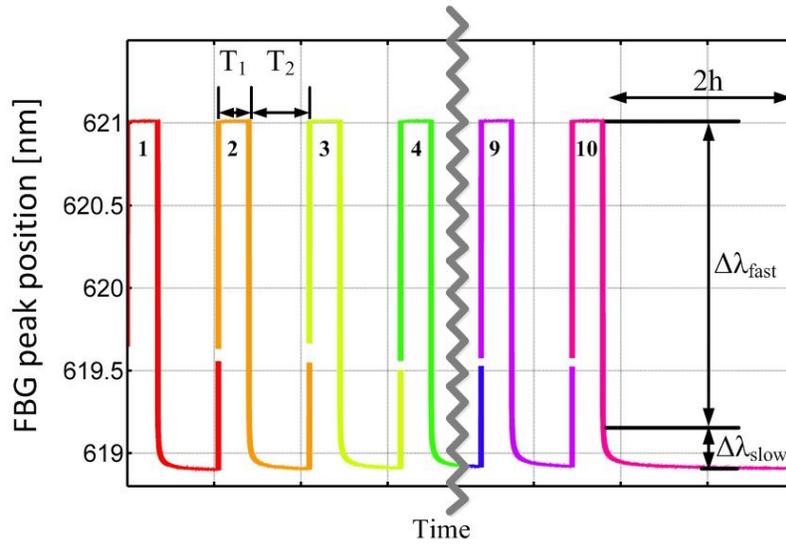

Figure 1. Scheme presenting one sequence of the experiment. For the same strain (here 0.5%) we strained the fiber for the duration T_1 after which the fiber was relaxed for the duration T_2. This cycle was repeated 10 times, after which the fiber was left relaxing for two hours to mitigate possible accumulated stress before the next experiment was conducted. In the right side of the figure the two main relaxation ranges are indicated: the elastic driven fast relaxation range $\Delta\lambda_{FAST}$, followed by the viscous dominated slow relaxation range $\Delta\lambda_{SLOW}$. $\Delta\lambda_{FAST}$ is defined as the FBG wavelength range where the fiber is following the strain applied by the motor (which is rapidly decreasing). $\Delta\lambda_{SLOW}$ is defined as the range in which the fiber does not follow the (rapidly decreasing) strain anymore but has a time lag, and the speed of the FBG peak shift has become 20 times slower.

Subsequently we repeated the 10-cycle strain-relaxation sequence 4 times with different values of the strain time T_1 (2.5, 5, 10 and 50 minutes) while we kept the fiber relaxation time T_2 at 5 minutes. After each 10-cycle sequence the fiber was left relaxing for 2 hours. The resulting 10 curves (forming a sequence) can be seen overlaid one over another in Figure 2.
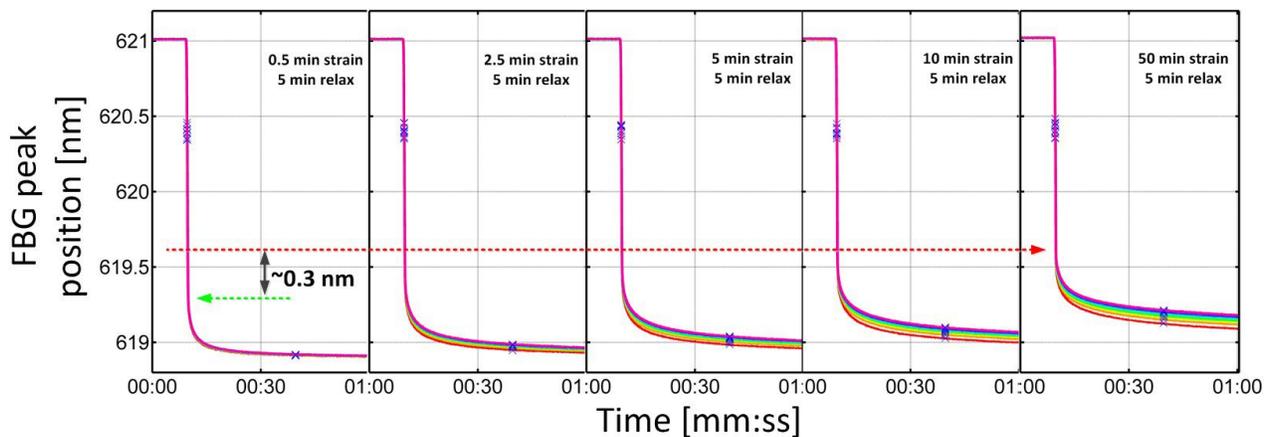

Figure 2. Evolution of the strain-relaxation cycle for a strain level of 0.5%. Each of the 5 windows is presenting 10 overlaid cycles forming one sequence of experiment, as presented in Figure 1. The straining time T_1 in the 5 windows is 0.5 min, 2.5 min, 5 min, 10 min, and 50 min, respectively, while the relaxation time T_2 was kept constant at 5 min. Positions marked with X are 30 seconds apart and were used for assessment of any changes in the cyclic behavior and appearance of hysteresis (see Fig. 4). It is visible that with increasing strain duration and for the same amount of strain, the fiber will take longer time to relax. The wavelength range $\Delta\lambda_{FAST}$, over which we can expect fast fiber contraction, decreased by 0.3 nm (shown as the difference between the dashed green and red arrows) when the strain duration was increased from 0.5 min to 5 min, thereby reducing the range of fast contraction $\Delta\lambda_{FAST}$ by about 18%.

We can see that in the low-strain regime (0.5%), relaxation for 5 minutes is enough for a complete relaxation of the fiber and the sequence shows almost no hysteresis. When increasing the duration of the strain we see appearance of hysteresis as it is visible that the relaxation time changes - it takes longer time for the fiber to relax.

2.2 Strain of 1%

The same experiment as in 2.1 was performed for a higher strain of 1% and the data are presented in Figure 3. For this higher strain, even for low strain-relaxation time ratios there is a small degree of hysteresis visible but in overall the fast relaxing region $\Delta\lambda_{FAST}$ is almost unchanged. That gives the strain of 1% a much bigger dynamic range $\Delta\lambda_{FAST}$ in comparison to 0.5% strain for short strain times (0.5 min). When increasing the strain duration, the hysteresis becomes more apparent and quite bigger than for a strain of 0.5%, as the fiber is taking even longer time to relax.
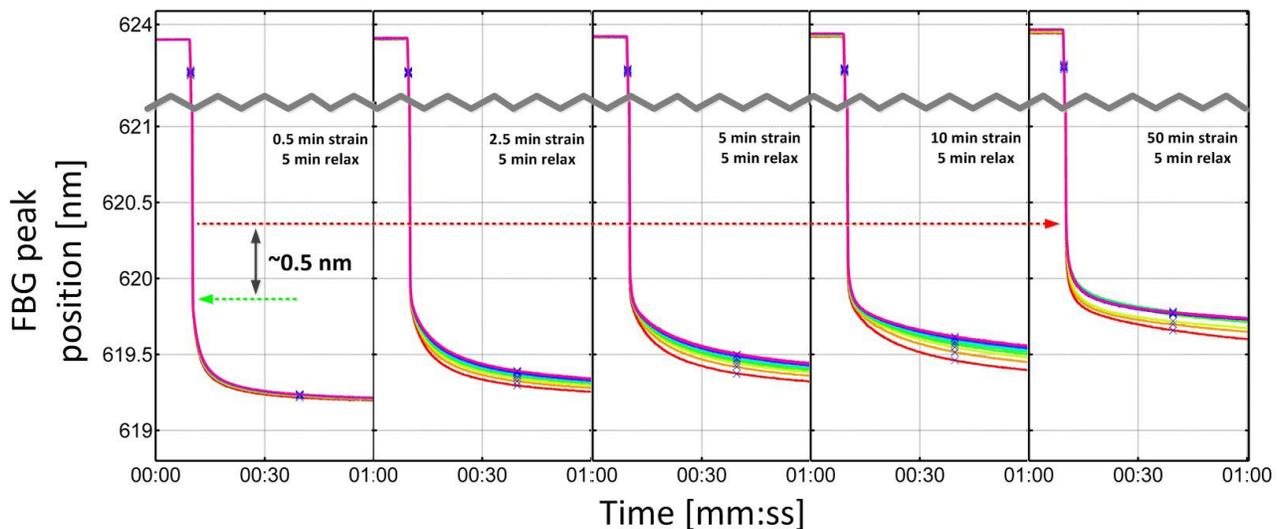

Figure 3. Evolution of the strain-relaxation cycle for a strain level of 1%. The experiment was performed the same way as described in Figure 1, but with strain of 1%. The wavelength range $\Delta\lambda_{FAST}$, over which we can expect fast fiber contraction, is decreased by 0.5 nm (shown as difference between dashed green and red arrows) when the strain duration was increased from 0.5 min to 5 min, thereby reducing the range of fast contraction $\Delta\lambda_{FAST}$ by about 13%. Positions marked with X are 30 seconds apart and were used for assessment of the change in hysteresis presented in Figure 4.

2.3 Hysteresis evolution for 0.5% and 1%

To assess the evolution of hysteresis, we monitored the relaxation curve 30 seconds after the fiber started relaxing (the two positions, start of relaxation and 30 seconds after, are marked with X in Figure 2 and Figure 3). In Figure 4 (a) and (b), it is visible that for the shortest strain time T_1 the fiber can follow the strain cycle and no significant hysteresis is visible. In other words, the FBG center wavelength after each cycle is constant.

With increasing strain duration T_1, the accumulated strain cannot be relaxed within 5 minutes of relaxation, so it influences the subsequent cycle. That manifests itself in the appearance of hysteresis, leading to an increase in the FBG wavelength floor rising logarithmically. For longer T_1, the relaxation equilibrium (constant FBG wavelength) is not reached within 10 cycles. For shorter T_1, it seems like the fiber needs a couple of more cycles to reach the relaxation equilibrium. Perhaps the most apparent observation in comparing 0.5% and 1% strain is the big offset in the FBG wavelength measured after 30 seconds. They are different by 0.3 nm, which corresponds to about 0.1% strain. While the FBG wavelength measured 30 seconds after the strain is higher for 1% strain, the overall fast relaxation range $\Delta\lambda_{FAST}$ is much bigger.

Looking at Fig. 4(b) and the graph for 50 minutes strain (green color), the curve is not smooth as the other ones. This is mainly due to a drift in our, otherwise humidity and temperature controlled environment.
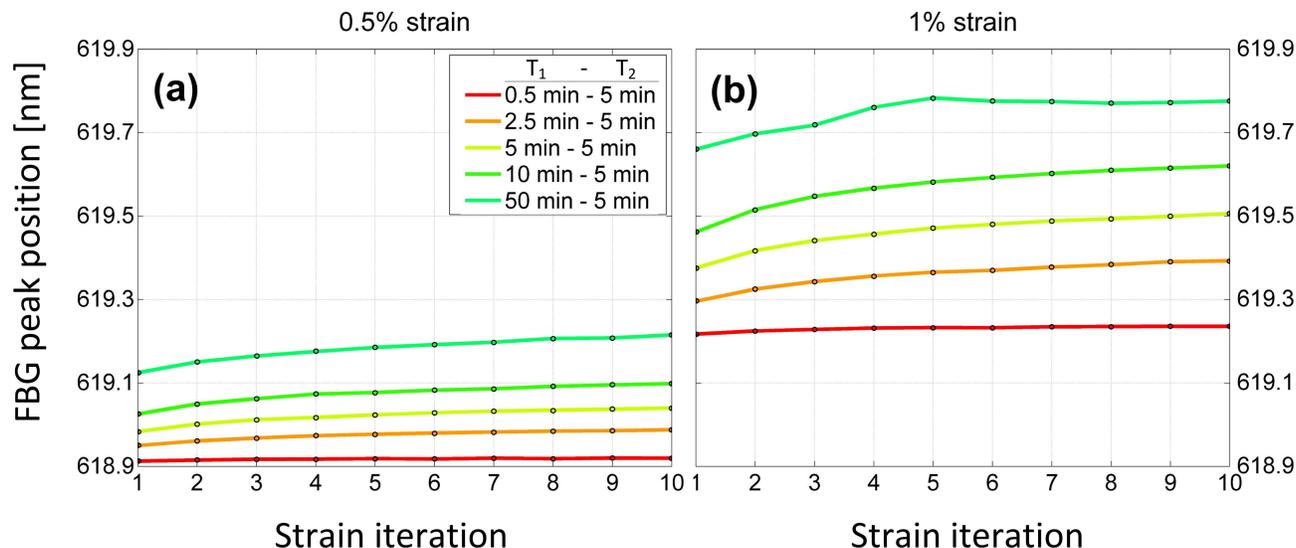
Figure 4. Relaxation hysteresis evolution for the point 30 seconds after the strain is released (see X marks on Fig. 2 and Fig. 3), for 0.5% (a) and 1% strain (b). For the 10 cycles of 0.5% strain shown in (a), we can see that for smaller T_1, the nearly negligible hysteresis is stabilized fairly quickly. For longer T_1, we observe a logarithmic evolution of the hysteresis, with the FBG wavelength still increasing after 10 cycles, even though it seems to be very close to the final value. The same behavior can be observed for 1% strain in (b). The green curve in the (b), representing a strain time of 50 minutes, seems uneven with respect to other curves, which is due to a drift of the temperature in the otherwise stabilized temperature chamber.

3. CONCLUSION

While having several advantageous properties, polymer fibers exhibit viscoelasticity, which makes them more demanding to implement in certain types of sensor applications. Depending on the amount of strain and the duration of the strain – the fiber relaxation will be different and hysteresis may appear if the relaxation time is not long enough. We have shown that the mainly viscous relaxation region increases with the strain duration and the strain amount. For a relaxation time of 5 minutes, it can amount to the strain of 0.3%, after the fiber has been strained for 50 minutes at 1% strain. We have also demonstrated that any appearing hysteresis will settle to equilibrium after a certain number of cycles, meaning that the relaxation behavior becomes identical for each of the following strain-relax cycles.

[1]   Stefani, A., Andresen, S., Yuan, W.., Bang, O., "Dynamic characterization of polymer optical fibers," IEEE Sens. J. **12**(10), 3047–3053 (2012).

[2]   Sáez-Rodríguez, D., Nielsen, K., Bang, O.., Webb, D. J., "Time-dependent variation of Fibre Bragg Grating Reflectivity in PMMA based Polymer Optical Fibres," Opt. Lett. (2015).

[3]   Stefani, A., Andresen, S., Yuan, W., Herholdt-Rasmussen, N.., Bang, O., "High sensitivity polymer optical fiber-Bragg-grating-based accelerometer," Photonics Technol. Lett. IEEE **24**(9), 763–765 (2012).

[4]   Yuan, W., Stefani, A.., Bang, O., "Tunable polymer fiber Bragg grating (FBG) inscription: Fabrication of dual-FBG temperature compensated polymer optical fiber strain sensors," IEEE Photonics Technol. Lett. **24**(5), 401–403 (2012).

[5]   Stefani, A., Nielsen, K., Rasmussen, H. K.., Bang, O., "Cleaving of TOPAS and PMMA microstructured polymer optical fibers: Core-shift and statistical quality optimization," Opt. Commun. **285**(7), 1825–1833, Elsevier B.V. (2012).